engineered restriction sites were inserted into the cloning plasmid pJF119EH1[20] both separately or in tandem. Cloning sites were *Bam*HI and *Pst*I for *entB*, and *Sac*I and *Bam*HI for *entC*, respectively. The *E. coli* strains W3110, DH5α, AN193, and H1882 were transformed with each of the resulting three plasmids.

Fermentations for product formation analysis were performed in a mineral salts medium (100 mL; pH 7 maintained by addition of 1N NaOH)[10] in 1 L shake flasks. Cells from a 100 mL preculture in Luria–Bertani medium[21] (containing 100 mg L^{-1} ampicillin, 100 μM isopropyl β-D-thiogalactopyranoside (IPTG) at an optical density ($\lambda = 600$ nm) of 2) were harvested in the mid-logarithmic phase and were resuspended in mineral salts medium (containing 100 mg L^{-1} ampicillin, 100 μM IPTG) and were incubated at 37 °C and 150 rpm. Product formation was monitored during a period of 10 h by HPLC analysis (maximal excretion was after ca. 4 h).

Mineral salts medium for optimized production and growth (derived from Pan et al.[16]) contained per liter: KH_2PO_4 (13 g), K_2HPO_4 (10 g), $NaH_2PO_4 \cdot 2H_2O$ (6 g), $(NH_4)_2SO_4$ (2 g), $MgSO_4 \cdot 7H_2O$ (3 g), NH_4Cl (5 g), $FeSO_4 \cdot 7H_2O$ (40 mg), $CaCl_2 \cdot 2H_2O$ (40 mg), $MnSO_4 \cdot 2H_2O$ (10 mg), $ZnSO_4 \cdot 7H_2O$ (2 mg), $AlCl_3 \cdot 6H_2O$ (10 mg), $CoCl_2 \cdot 6H_2O$ (4 mg), $Na_2MoO_4 \cdot 2H_2O$ (2 mg), $CuCl_2 \cdot 2H_2O$ (1 mg), H_3BO_3 (0.5 mg), leucine (200 mg), proline (200 mg), adenine (200 mg), thiamine (20 mg), tryptophan (200 mg), 2,3-dihydroxybenzoic acid (20 mg), and ampicillin (100 mg).

The cultivation in a 30 L stirred tank bioreactor (Chemap, Switzerland, 20 L working volume) was performed at pH 6.8 (controlled) and 37 °C with optimized medium. 1 L preculture from complex medium served as inoculum. The initial concentration of glucose was 30 g L^{-1}. The carbon source was added in portions so that the concentration was maintained in the range of 5–10 g L^{-1}. Induction by addition of 100 μM (final concentration) IPTG was at a cell concentration of 5 g L^{-1} (dry cell mass). The aeration rate was regulated to 25 L min^{-1}(air).

The crude product was purified by column chromatography on silica gel 60 using ethyl acetate/MeOH (5/1) as eluent. Physical data of **3** (yellow solid): $[\alpha]_D^{20} = 3.8$ ($c = 0.6$ in ethanol); ^{1}H NMR (300 MHz, [D$_4$]MeOH, 23 °C): $\delta =$ 4.10 (d, ^3J(H,H) = 2.5 Hz, 1H; C*H*OH), 4.50 (d, ^3J(H,H) = 2.5 Hz, 1H; C*H*OH), 6.20 (m, 2H; C=C*H*), 7.06 (dd, ^3J(H,H) = 3.3 Hz, ^4J(H,H) = 3.2 Hz, 1H; C=C*H*); ^{13}C NMR (75 MHz, [D$_4$]MeOH, 23 °C): $\delta = 68.8$ (CH), 70.4 (CH), 125.1 (CH), 130.8 (C_{quart}), 134.3 (CH), 134.4 (CH), 170.2 (COOH); IR(KBr): $\tilde{\nu} = 1699$ cm^{-1} (C=O), 1644 (C=C), 1586 (C=C), 1258, 1075, 1008; UV/Vis (H_2O): $\lambda_{max}(\varepsilon) = 279$ nm (4900); EI-MS (70 eV): *m*/*z* (%): 156 (6) [M^+], 138 (100) [$M^+ - H_2O$], 110 (63) [$M^+ - 2H_2O$], 93 (10), 82 (29), 65 (13) [$C_5H_5^+$]; HR-MS: calcd for $C_7H_8O_4$: 156.0423; found: 156.0424.

Received: August 31, 2000 [Z15735]

[1] Overviews: a) S. M. Brown, T. Hudlicky in *Organic Synthesis: Theory and Applications*, *Vol. 2* (Ed.: T. Hudlicky), JAI, New York, **1993**, pp. 113–176; b) T. Hudlicky, J. W. Reed in *Advances in Asymmetric Synthesis*, *Vol. 1* (Ed.: A. Hassner), JAI, New York, **1995**, pp. 271–312; c) T. Hudlicky, D. Gonzalez, D. T. Gibson, *Aldrichimica Acta* **1999**, *32*, 35–62, and references therein.

[2] H. A. J. Carless, *J. Chem. Soc. Chem. Commun.* **1992**, 234–235.

[3] T. Hudlicky, G. Seoane, T. Pettus, *J. Org. Chem.* **1989**, *54*, 4239–4243.

[4] G. Butora, T. Hudlicky, S. P. Fearnley, M. R. Stabile, A. G. Gum, D. Gonzalez, *Synthesis* **1998**, 665–681.

[5] a) T. K. M. Shing, E. K. W. Tam, *Tetrahedron: Asymmetry* **1996**, *7*, 353–356; b) B. M. Trost, L. S. Chupak, T. Lübbers, *J. Am. Chem. Soc.* **1998**, *120*, 1732–1740.

[6] Following a synthetic route of Trost et al.[5b] and starting with methyl propiolate and crotonaldehyde we synthesized racemic **3** in six reaction steps and 14% overall yield.[19]

[7] a) D. R. Boyd, N. D. Sharma, H. Dalton, D. A. Clarke, *Chem. Commun.* **1996**, 45–46; b) B. P. McKibben, G. S. Barnosky, T. Hudlicky, *Synlett* **1995**, 806–807; c) D. R. Boyd, N. D. Sharma, C. R. O'Dowd, F. Hempenstall, *Chem. Commun.* **2000**, 2151–2152.

[8] T. K. M. Shing, E. K. W. Tam, *J. Org. Chem.* **1998**, *63*, 1547–1554.

[9] K. M. Draths, D. R. Knop, J. W. Frost, *J. Am. Chem. Soc.* **1999**, *121*, 1603–1604.

[10] R. Müller, M. Breuer, A. Wagener, K. Schmidt, E. Leistner, *Microbiology* **1996**, *142*, 1005–1012.

[11] C. F. Earhart in *Escherichia coli and Salmonella*, *Vol. 1* (Ed.: F. C. Neidhardt), 2nd ed., ASM, Washington, DC, **1996**, pp. 1075–1090.

[12] D. Hanahan, *J. Mol. Biol.* **1983**, *166*, 557–580.

[13] a) C. W. Hill, B. W. Harnish, *Proc. Natl. Acad. Sci. USA* **1981**, *78*, 7069–7072; b) K. F. Jensen, *J. Bacteriol.* **1993**, *175*, 3401–3407.

[14] a) G. B. Cox, F. Gibson, R. K. J. Luke, N. A. Newton, I. G. O'Brion, H. Rosenberg, *J. Bacteriol.* **1970**, *104*, 219–226; b) B. A. Ozenberger, T. J. Brickman, M. A. McIntosh, *J. Bacteriol.* **1989**, *171*, 775–783.

[15] a) M. J. Casadaban, *J. Mol. Biol.* **1976**, *104*, 541–555; b) M. J. Casadaban, S. N. Cohen, *Proc. Natl. Acad. Sci. USA* **1979**, *76*, 4530–4533; c) Y. Komeda, T. Iino, *J. Bacteriol.* **1979**, *139*, 721–729.

[16] J. G. Pan, J. S. Rhee, J. M. Lebeault, *Biotechnol. Lett.* **1987**, *9*, 89–94.

[17] With regard to the theoretical maximum yield the relative molar yield was 40%; K. Li, J. W. Frost, *Biotechnol. Prog.* **1999**, *15*, 876–883.

[18] M. Halfar, J. Thömmes, D. Franke, M. Müller, unpublished results.

[19] V. Lorbach, D. Franke, M. Müller, unpublished results.

[20] J. P. Fürste, W. Pansegrau, R. Frank, H. Blöcker, P. Scholz, M. Bagdasarian, E. Lanka, *Gene* **1986**, *48*, 119–131.

[21] J. Sambrook, E. F. Fritsch, T. Maniatis, *Molecular Cloning: A Laboratory Manual*, 2nd ed., Cold Spring Harbor, NY, **1989**.

On the Aromatic Character of Electrocyclic and Pseudopericyclic Reactions: Thermal Cyclization of (2*Z*)-Hexa-2,4-5-trienals and Their Schiff Bases**

Angel R. de Lera,* Rosana Alvarez, Begoña Lecea, Alicia Torrado, and Fernando P. Cossío*

Recent research on the magnetic characterization of aromaticity[1] has, over the last few years, promoted the reexamination of the aromatic character of pericyclic reactions.[2] This idea stems from the pioneering work of Evans,[3a] Dewar,[3b] and Zimmerman[3c] and has been refined by Herges, Jiao, and Schleyer.[2] Recently, we reported[4] that the concept of in-plane (σ) aromaticity can be extended to several thermal pericyclic reactions. Within this context, we herein report several ring closures involving (2*Z*)-hexa-2,4,5-trienals and their corresponding imines (Scheme 1). These compounds are

[*] Prof. Dr. A. R. de Lera, Dr. R. Alvarez, Dr. A. Torrado
Departamento de Química Orgánica
Universidade de Vigo
36200 Vigo (Spain)
Fax: (+34) 86-812382
E-mail: qolera@correo.uvigo.es

Prof. Dr. F. P. Cossío, Prof. Dr. B. Lecea
Kimika Fakultatea
Euskal Herriko Unibertsitatea
P.K. 1072 20080 San Sebastián-Donostia (Spain)
Fax: (+34) 43-212236
E-mail: qopcomof@sq.ehu.es

[**] This work was supported by the Spanish Ministerio de Investigación (Grant no.: SAF98-0143), by the Xunta de Galicia (Grant no.: PGIDT99PXI30105B), by the Eusko Jaurlaritza (Grant nos.: EX1998-126 and PI1998-116), by Gipuzkoako Foru Aldundia, and by Fondo de Cooperación Aquitania-Euskadi. We thank Dr. J. Rodriguez-Otero and Dr. S. Lopez (Universidade de Santiago) for helpful discussions.

Supporting information for this article is available on the WWW under http://www.angewandte.com or from the author.

  1433-7851/01/4003-0557 $ 17.50+.50/0

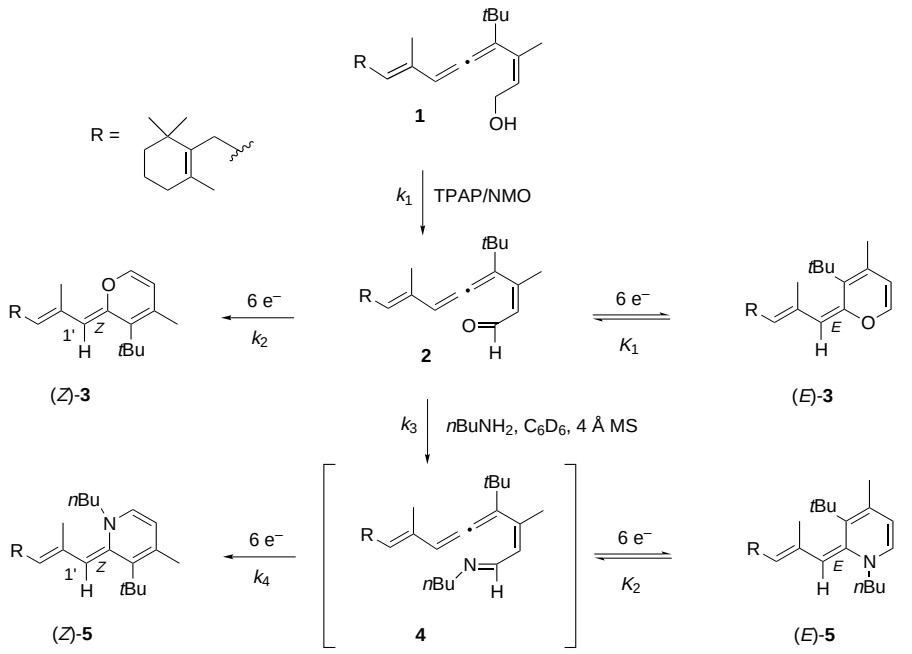

Scheme 1. Synthesis and cyclization of the (2*Z*)-hexa-2,4,5-trienal **2** and its *N*-butyl Schiff base **4**. TPAP = tetrapropylammonium perruthenate, NMO = 4-methylmorpholine *N*-oxide, MS = molecular sieves.

interesting model systems for the study of the chemistry of cumulenes and retinoids.[5] A common feature of these systems is the presence of a cumulene bond and a heteroatom at one end of the interacting system. This electronic array allows for either one or two orbital disconnections, that is, regions where orthogonal sets of orbitals meet but do not overlap at the transition state associated with their cyclization (see Scheme 2). This situation constitutes a common feature of a subset of pericyclic reactions termed pseudopericyclic.[6]

We have observed the facile electrocyclic ring closure of (2*Z*)-hexa-2,4,5-trienal **2** to alkylidene-2*H*-pyran **3**, which proceeds at room temperature upon oxidation of precursor (2*Z*)-hexa-2,4,5-trienol **1** (Scheme 1).[7] Detailed kinetic analysis[8] of the depicted transformation revealed that the divinylallenal **2**, obtained by oxidation of **1** with TPAP and NMO, experienced fast equilibration with the kinetically favored cyclized product, alkylidene-2*H*-pyran (*E*)-**3**, by a process which was interpreted as a sequence of electrocyclic ring-closure and electrocyclic ring-opening reactions. In contrast, the alternative cyclization of **2** leading to the thermodynamically most stable alkylidene-2*H*-pyran (*Z*)-**3** was irreversible. This isomer accumulated in the reaction mixture, becoming the only component after about 48 hours. We also carried out a similar study with the imine derivative. In order to minimize the competing O→C cyclization, the residue obtained upon oxidation was immediately treated with *n*-butylamine (2.0 equiv) in C_6D_6 in the presence of 4 Å molecular sieves. The reaction progress was followed by ^{1}H NMR spectroscopy.[8] Upon standing in solution, the ^{1}H NMR spectra revealed the presence of only two components in a 93:7 ratio after 6 h (no change was detected upon doubling the reaction time). The minor component was identified as the previously characterized[8] alkylidene-2H-pyran (*Z*)-**3**. The major component was shown to be its nitrogen analogue, the *N*-butylalkylidenepyridine (*Z*)-**5**, which originates from the intermediate Schiff base **4**. Despite the fact that diagnostic signals (the imine hydrogen signal) for the putative Schiff base **4** were not detected in the ^{1}H NMR spectra throughout the entire experiment, it was considered likely to be an intermediate en route to (*Z*)-**5**. Moreover, close examination of the ^{1}H NMR spectra at low conversions indicates the presence of signals similar to those of (*Z*)-**5**, which decreased in intensity with time. By analogy to the O→C cyclization, those signals were interpreted as due to the kinetically favored (*E*)-alkylidenepyridine (*E*)-**5** in equilibrium with the putative Schiff base **4**. The cyclization of the imine **4** to (*Z*)-**5** must be irreversible under the reaction conditions, in keeping with the irreversibility of the competing cyclization of **2** to (*Z*)-**3**, but the former is more favorable. The rate constants for the N→C cyclization were shown to be higher than those of the O→C cyclization regardless of the solvent used (see below). The ^{1}H NMR spectroscopic monitoring and the kinetic analysis did not reveal the intervention of alternative mechanism(s) for the direct conversion of (*Z*)-**3** into (*Z*)-**5**, since heating a solution of isolated (*Z*)-**3** in C_6D_6 to 50 °C with excess $nBuNH_2$ led to the recovery of unaltered (*Z*)-**3**.

In order to understand the mechanistic nature of the above transformations, we have selected the model reactions A–C, the cyclizations of **6a–c** into **7a–c** (Scheme 2). These

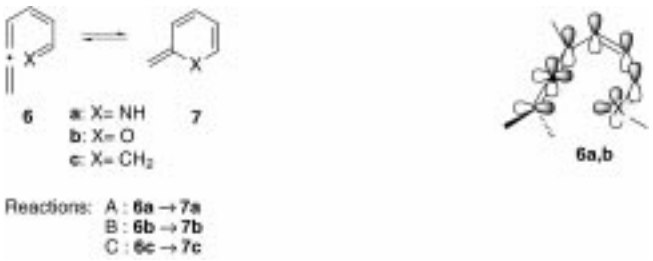

Scheme 2. The model reactions A–C.

reactions can proceed through two possible mechanisms. The first, denoted as (a) in Scheme 3, consists of a disrotatory thermal electrocyclization via the transition state **TS**. The second mechanism, denoted as (b) in Scheme 3 involves a nucleophilic addition of the heteroatom lone pair onto the sp-hybridized carbon atoms of **6a** and **6b**. According to this latter mechanism an appreciable negative charge at the exocyclic carbon atom of **TS′** should be expected. This latter mechanism consists of a pseudopericyclic process since orbital symmetry is not involved and the corresponding transition structure must be planar or nearly planar.[6b–f]

  1433-7851/01/4003-0558 $ 17.50+.50/0 *Angew. Chem. Int. Ed.* **2001**, *40*, No. 3

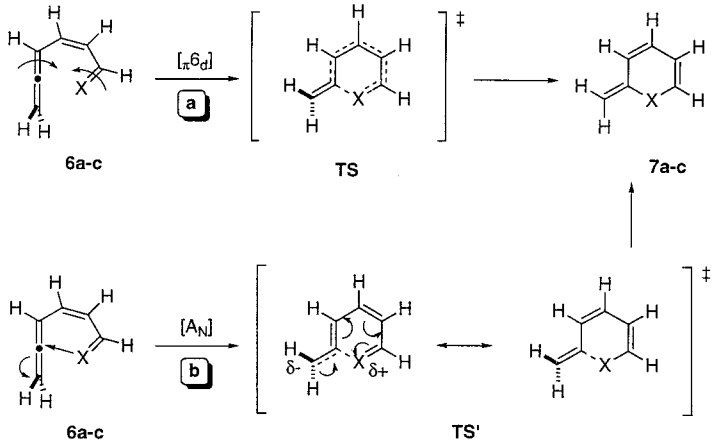

Scheme 3. Mechanisms of the disrotatory thermal electrocyclization (a) and the pseudopericyclic reaction (b).

We have computed the reaction profile associated with the **6a–c**→**7a–c** transformations at the B3LYP/6–31+G*+ΔZPVE level.[9] In all cases, we have found only one transition structure connecting both stationary points. The chief features of **TSa–c** are depicted in Figure 1. The

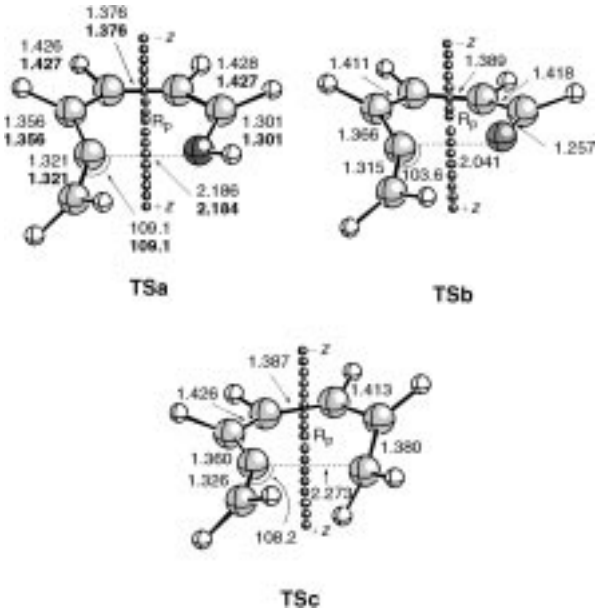

Figure 1. Main geometric features of **TSa–c** computed at the B3LYP/6–31+G* (numbers printed in normal text) and B3LYP(SCIPCM)/6–31+G* (in toluene; bold numbers) levels. Lengths and angles are given in Å and degrees, respectively. R_p stands for the (3,+1) ring point of electron density. The small spheres correspond to the points used in the evaluation of the NICS values (see text).

harmonic analysis of **TSa** reveals that the nuclear motion corresponding to the imaginary frequency of its diagonalized Hessian matrix has no component associated with rotation of the N1–H group with respect to the N1–C2 bond being formed. Instead, aside from indicators for a N1···C2 stretching interaction, there is a component associated with rotation of the exocyclic H–C7 groups with respect to the C2–C7 bond. This rotation corresponds to the rehybridization of the C2 atom and therefore is not associated with disrotatory motion. In addition, the natural bond orbital (NBO) analysis reveals a charge of −0.22 e at the C7 atom, a value in agreement with the electron distribution expected for the structure of **TS′**. All these data indicate that the mechanism of this reaction is the nucleophilic addition depicted in pathway (b) of Scheme 3. **TSb** exhibits similar geometric and electronic features, except that in this case the oxygen atom does not have any substituents so the absence of rotation around the O1–C2 bond cannot be observed in the corresponding imaginary frequency. In contrast, **TSc** exhibits disrotatory motion in its imaginary frequency, as well as no significant charge redistribution.

We have also tested the dependence of the activation barriers of reactions A–C with the polarity of the solvent. The results are reported in Table 1. All three model trans-

Table 1. Distance R_0 [Å] of the aromaticity with an average radius R_{av} [Å], maximum NICS values[a] [ppm mol^{-1}], maximum diamagnetic shieldings[b] σ^d_{max} [ppm mol^{-1}], and activation energies[c] ΔE_a [kcal mol^{-1}] for transition structures **TSa–c**, as well as the reaction energies[c] ΔE_{rxn} [kcal mol^{-1}] for reactions A–C.

Parameter	TSa	TSb	TSc
R_0	0.60	0.76	0.38
R_{av}	1.35	1.20	1.25
$NICS_{max}$	−7.75	−6.80	−13.64
σ^d_{max}	−10.44	−11.74	−11.57
ΔE_a ($\varepsilon = 1.00$)	6.4	8.6	17.4
ΔE_a ($\varepsilon = 3.39$)	6.3	9.0	17.4
ΔE_a ($\varepsilon = 20.56$ (acetone))	6.2	9.4	17.6
ΔE_{rxn} ($\varepsilon = 1.00$)	−40.6	−22.1	−29.1

[a] Calculated at the B3LYP-GIAO/6–31+G* level. [b] Calculated according to Equations (1) and (2). [c] Calculated at the B3LYP/6–31+G*+ΔZPVE and B3LYP(SCIPCM)/6–31+G*//B3LYP(L1A1)/6–31+G*+ΔZPVE levels.

formations exhibit low solvent effects. In reactions B and C the activation energies increase when the polarity of the solvent increases. In the case of reaction A, the polarity of **TS′a**, as well as the ability of the nitrogen atom to accommodate the partial positive charge, accounts for the lowering of the activation energy with the polarity of the solvent. These predictions were corroborated experimentally: Solutions of aldehyde **2**, prepared as described above, in different deuterated solvents were treated with nBuNH$_2$ (1.1 mol equiv) in the presence of 4 Å molecular sieves, and ^{1}H NMR spectra were measured at room temperature to determine rate constants. Figure 2 depicts the dependence of the experimentally determined reaction rates on the polarity of the solvent according to the E_N^T (normalized empirical solvent polarity) parameter.[10] Similar linear plots were obtained when ln$k$ was represented against the Onsager function $(\varepsilon-1)/(2\varepsilon+1)$, with slopes of opposite sign obtained for the **2**→**3** and **4**→**5** cyclizations.

We have also investigated the aromatic character of **TSa–c** by computing the nucleus-independent chemical shifts (NICS)[11] at the (3,+1) ring critical point of electron density as defined by Bader.[12] In general, large negative NICS values are associated with aromatic character.[1b, 11] We report in Figure 3 the NICS values computed along the z-axis defined by the points depicted in Figure 1. The NICS values along the

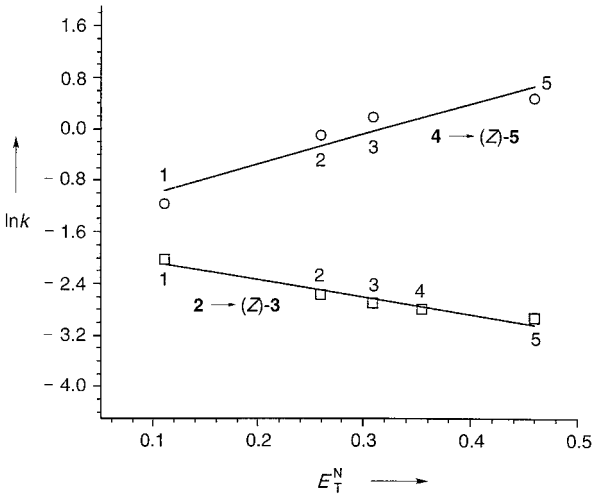

Figure 2. Plot of ln$k$ versus the solvent parameter E_T^N for the electrocyclizations **2**→**3** and **4**→**5**. 1: Benzene ($E_T^N = 0.111$), 2: chloroform ($E_T^N = 0.259$), 3: dichloromethane ($E_T^N = 0.309$), 4: acetone ($E_T^N = 0.355$), 5: acetonitrile ($E_T^N = 0.460$). Rate constants [h^{-1}] for the **2**→**3** and **4**→**5** reactions, respectively: in benzene: 0.13 (±0.02) and 0.31 (±0.02), in chloroform: 0.08 (±0.01) and 0.90 (±0.10), in dichloromethane: 0.07 (±0.01) and 1.19 (±0.11), in acetone 0.05 (±0.01) and not determined, acetonitrile 0.05 (±0.01) and 1.61 (±0.09).

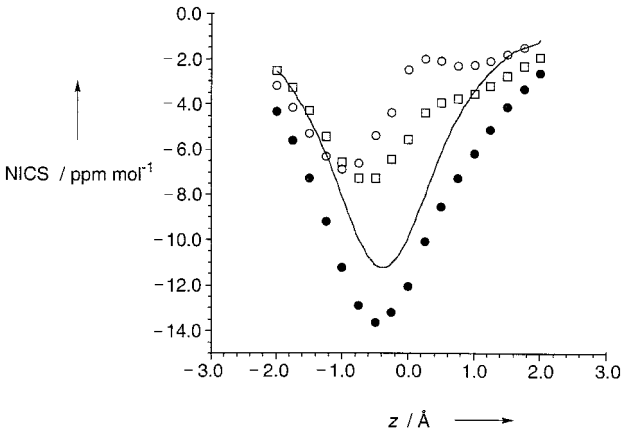

Figure 3. Plot of the calculated NICS versus z for transition structures **TSa** (□), **TSb** (○), and **TSc** (●). The NICS values have been obtained at the GIAO-SCF/6 – 31G*//B3LYP/6 – 31G* level. The z axis has been defined as depicted in Figure 1. The continuous line is the σ_{zz}^d versus z curve for **TSc**, calculated with Equations (1) and (2) and the values reported in Table 1.

z-axis in pseudopericyclic reactions A and B are different to those computed for the electrocyclic reaction C. In **TSa**, **b** the $NICS_{max}$ values are significantly less negative than for **TSc** (Table 1). In addition, for reaction C the NICS values decrease in negativity monotonously along the z-axis in the region $z > R_0$, whereas in **TSa**, **b** they do not. Indeed, in **TSb** a second local negative maximum (in absolute value) is reached at $z = 0.8$ Å (See Figure 3).

We have previously demonstrated[4] that the aromatic character of one given transition structure or stable molecule can be described by means of the ring current model. In general, for a ring current of R_{av} radius and circulating at a certain distance R_0 above the average molecular plane, the variation of the diamagnetic shielding σ_{zz}^d along the axis perpendicular to such a plane can be described by Equations (1) and (2). In these equations σ_{max}^d stands for the maximum (absolute value) diamagnetic shielding.

$$\sigma_{zz}^d = \sigma_{max}^d \left[1 + \left(\frac{z - R_0}{R_{av}}\right)^2\right]^{-3/2} \quad (1)$$

$$\sigma_{max}^d = -\frac{e^2 \mu_0}{8\pi m_e} R_{av}^{-1} \quad (2)$$

As shown in Table 1, the σ_{max}^d value obtained for **TSc** is similar, although slightly smaller, than the corresponding $NICS_{max}$ value. Moreover, the variation of the NICS and the σ_{zz}^d values along the z-axis is similar in both cases (Figure 3). This indicates that the ring current model accounts for approximately 85% of the total diamagnetic shielding observed in **TSc**, and that local effects do not vary significantly along the z-axis. Thus we can conclude that **TSc** is aromatic. In contrast, in both **TSa**, **b** neither the $NICS_{max}$ values nor the variation of the NICS and σ_{zz}^d values along the z-axis agree with the behavior described by Equations (1) and (2). In addition, the $NICS_{max}$ values are lower than those predicted by the ring current model for σ_{zz}^d. These results indicate that in both **TSa**, **b** the diamagnetic effects reported in Figure 3 and in Table 1 are due to local effects induced by the heteroatoms and π bonds.

The ring current model and the magnetic criteria permit a clear distinction between disrotatory electrocyclic reactions, which are associated with aromatic structures, and pseudopericyclic reactions, which are not. We can therefore confirm the suggestion we made in previous papers[4] that the behavior of the diamagnetic shielding along the axis perpendicular to the average molecular plane is useful for distinguishing between different types of aromaticity. Thus, in σ aromaticity there is a maximum diamagnetic shielding at the ring point of electron density (Figure 4). This kind of aromaticity is found in highly planar transition structures involving formation of σ bonds, for example in [3+2] and [2+2+2] cycloadditions. In contrast, in the usual π aromaticity the maximum diamagnetic shielding takes place at a certain distance above *and* below the

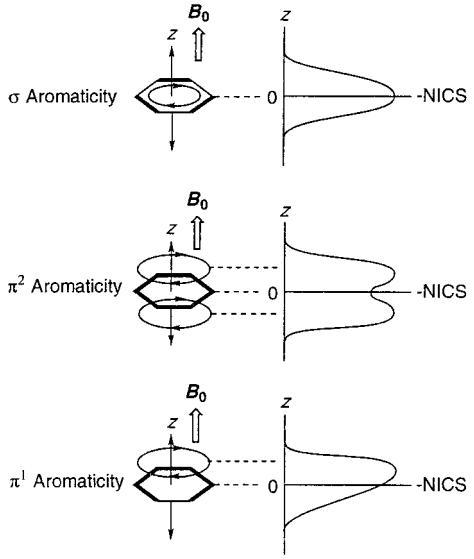

Figure 4. Schematic definition of different types of aromaticity according to the behavior of the diamagnetic shielding along the axis perpendicular to the molecular plane and containing the ring point of electron density.

  1433-7851/01/4003-0560 $ 17.50+.50/0 *Angew. Chem. Int. Ed.* **2001**, *40*, No. 3

molecular plane (Figure 4). This effect can be described by means of two ring currents circulating at a certain distance of the molecular plane. In this paper, instead, we have observed one highly aromatic disrotatory ring closure in which there is only one maximum diamagnetic shielding above the molecular plane. In a formal sense this transition structure corresponds to π aromaticity involving only one ring current circulating on the side where the disrotatory movement allows a close proximity between the terminal p atomic orbitals (pAO). We therefore propose the terms π^1 aromaticity and π^2 aromaticity to describe these two different kinds of aromatic transition structures.

Received: July 4, 2000 [Z15386]

[1] a) T. M. Krygowski, M. K. Cyranski, Z. Czarnocki, G. Häfelinger, A. R. Katritzky, *Tetrahedron* **2000**, *56*, 1783; b) P. von R. Schleyer, H. Jiao, *Pure Appl. Chem.* **1996**, *68*, 209, and references therein; c) V. I. Minkin, M. N. Glukhovtsev, B. Y. Simkin, *Aromaticity and Antiaromaticity: Electronic and Structural Aspects*, Wiley, New York, **1994**, pp. 63–74.

[2] a) R. Herges, H. Jiao, P. von R. Schleyer, *Angew. Chem.* **1994**, *106*, 1441; *Angew. Chem. Int. Ed. Engl.* **1994**, *33*, 1736; b) H. Jiao, P. von R. Schleyer, *Angew. Chem.* **1995**, *107*, 329; *Angew. Chem. Int. Ed. Engl.* **1995**, *34*, 334; c) H. Jiao, P. von R. Schleyer, *J. Phys. Org. Chem.* **1998**, *11*, 655.

[3] a) M. G. Evans, *Trans. Faraday Soc.* **1939**, *35*, 824; b) M. J. S. Dewar, *The Molecular Orbital Theory of Organic Chemistry*, McGraw-Hill, New York, **1969**, pp. 316–339; c) H. Zimmerman, *Acc. Chem. Res.* **1971**, *4*, 272.

[4] a) F. P. Cossío, I. Morao, H. Jiao, P. von R. Schleyer, *J. Am. Chem. Soc.* **1999**, *121*, 6737; b) F. P. Cossío, I. Morao, *J. Org. Chem.* **1999**, *64*, 1868.

[5] B. Iglesias, A. Torrado, A. R. de Lera, S. López, *J. Org. Chem.* **2000**, *65*, 2696.

[6] a) J. A. Ross, R. P. Seiders, D. M. Lemal, *J. Am. Chem. Soc.* **1976**, *98*, 4325; b) D. M. Birney, P. E. Wagenseller, *J. Am. Chem. Soc.* **1994**, *116*, 6262; c) D. M. Birney, S. Ham, G. R. Unruh, *J. Am. Chem. Soc.* **1997**, *119*, 4509; d) D. M. Birney, X. L. Xu, S. Ham, X. M. J. Huang, *J. Org. Chem.* **1997**, *62*, 7114; e) D. M. Birney, X. Xu, S. Ham, *Angew. Chem.* **1999**, *111*, 147; *Angew. Chem. Int. Ed.* **1999**, *38*, 189; f) W. M. F. Fabian, C. O. Kappe, V. A. Bakulev, *J. Org. Chem.* **2000**, *65*, 47.

[7] A. R. de Lera, A. Torrado, J. García, S. López, *Tetrahedron Lett.* **1997**, *38*, 7421.

[8] See the Supporting Information for the detailed experimental procedures and the characterization of the cyclic compounds discussed in the text. The (*Z*)-alkylidene double-bond geometry of compound (*Z*)-**5** was based on the failure to observe an enhancement in the signal of the exocyclic $H_{1'}$ atom upon saturation of the $N-CH_2$ group, whereas the same signal was enhanced when the *t*Bu signal was irradiated. For structural comparison, stable bismerocyanines with alkylidenepyridine rings linked by a 1,8-naphthylene skeleton have recently been described, which show signals for the alkylidenepyridine ring similar to those of **5**: T. Katoh, Y. Inagaki, R. Okazaki, *J. Am. Chem. Soc.* **1998**, *120*, 3623.

[9] a) *Gaussian 98*, Revision A.5, Gaussian, Inc., Pittsburgh, PA, **1998**; b) B3LYP: A. D. Becke, *J. Chem. Phys.* **1993**, *98*, 5648; c) SCIPCM: J. B. Foresman, T. A. Keith, K. B. Wiberg, J. Snoonian, M. J. Frisch, *J. Phys. Chem.* **1996**, *100*, 16098; d) *NBO*, Version 3.1, E. D. Glendening, A. E. Reed, J. E. Carpenter, F. Weinhold; e) GIAO: K. Wolinski, J. F. Hilton, P. Pulay, *J. Am. Chem. Soc.* **1990**, *112*, 8251.

[10] C. Reichardt, *Solvents and Solvent Effects in Organic Chemistry*, VCH, Weinheim, **1990**, pp. 408–410.

[11] P. von R. Schleyer, C. Maerker, A. Dransfeld, H. Jiao, N. J. R. v. E. Hommes, *J. Am. Chem. Soc.* **1996**, *118*, 6317.

[12] R. F. W. Bader, *Atoms in Molecules—A Quantum Theory*, Clarendon, Oxford, **1990**, pp. 12–52.

Stereoselective Formation of C_2-Symmetric ansa-Lanthanocenes by Reductive Coupling of Acenaphthylene with Activated Ytterbium or Samarium**

Igor L. Fedushkin,* Sebastian Dechert, and Herbert Schumann*

Dedicated to Professor Jörn Müller on the occasion of his 65th birthday

C_2-symmetric ansa-metallocenes have been studied intensively because of their potential use as catalysts for stereoselective olefin polymerization processes.[1] Edelmann et al. and, later on, Shapiro et al. and Eisch et al. reported on a method to synthesize interannular ethano-bridged ansa-metallocenes by the reductive coupling of 6-substituted or 6,6′-disubstituted fulvenes with metallic calcium, lanthanide metals, or the dihalides of titanium and zirconium.[2] The reaction with 6-substituted fulvenes results in the formation of mixtures of *rac* and *meso* isomers. The exclusive formation of just one isomer by fulvene-type coupling has not yet been observed.[2e] The synthesis of ansa-metallocenes from bridged cyclopentadienyl dianions also produces only mixtures of isomers of variable *rac*:*meso* ratios.[3] We now suggest that the reductive coupling of a ligand in which the coupling exocyclic carbon atom of the fulvene moiety is fixed by incorporation into a condensed aromatic ring system such as in acenaphthylene (acene) would probably allow the isolation of an isomerically pure ansa-metallocene. Acene combines one five- and two six-membered rings and its resonance structures reveal the fulvene pattern. The only reductive coupling process of acene known so far is its reaction with $[V(CO)_6]$ which produces the double half-sandwich vanadium complex $(\mu_2\text{-}\eta^5\text{:}\eta^5\text{-}C_{24}H_{16})[V(CO)_4]_2$.[4] Here we report the reductive coupling of acene by activated metallic ytterbium and samarium, which yields the respective C_2-symmetric *trans*-*rac*-ansa-lanthanocenes.

The high electron affinity of acene ($E_{1/2} = -1.65$ V)[5] allows its reduction with activated metallic ytterbium or samarium, affording the ansa-lanthanocenes $[(\eta^5\text{-}C_{12}H_8)_2Ln(thf)_2]$ as dark red (Ln = Yb, **1**) or dark brown crystals (Ln = Sm, **2**) in yields of about 90% (Scheme 1). The ytterbium and samarium are activated by addition of iodine to the respective

[*] Dr. I. L. Fedushkin
G. A. Razuvaev Institute of Organometallic Chemistry of Russian Academy of Sciences
Tropinina 49, 603600 Nizhny Novgorod GSP-445 (Russia)
Fax: (+7) 8312-661497
E-mail: igorfed@imoc.sinn.ru
Prof. Dr. H. Schumann, Dipl.-Chem. S. Dechert
Institut für Anorganische und Analytische Chemie
Technische Universität Berlin
Strasse des 17. Juni 135, 10623 Berlin (Germany)
Fax: (+49) 30-3142-2168
E-mail: schumann@chem.tu-berlin.de

[**] Organometallic Compounds of the Lanthanides, Part 144. This work was supported by the Fonds der Chemischen Industrie, the Deutsche Forschungsgemeinschaft, and the Alexander von Humboldt foundation (research fellowship for I.L.F.). Part 143: M. Glanz, S. Dechert, H. Schumann, D. Wolff, J. Springer, *Z. Anorg. Allg. Chem.* **2000**, *626*, 2467–2477.